

**IDENTIFICATION OF ANTIMALARIAL
COMPOUNDS AND THEIR MODE OF ACTIONS**

FAUZE BIN MAHMUD

UNIVERSITI SAINS MALAYSIA

2022

IDENTIFICATION OF ANTIMALARIAL COMPOUNDS AND THEIR MODE OF ACTIONS

by

FAUZE BIN MAHMUD

**Thesis submitted in fulfilment of the requirements
for the degree of
Doctor of Philosophy**

October 2022

ACKNOWLEDGEMENT

I would like to express my sincere gratitude to my supervisors, especially Dr. Lai Ngit Shin (INFORMM, Universiti Sains Malaysia), Prof. Dr. Hiroyuki Osada, Dr. Yushi Futamura (CBRG, RIKEN, Japan), and Prof. Dr. Lee Ping Chin (FSSA, Universiti Malaysia Sabah), for believing in my research and passion for malaria study. Their support and brilliant advice helped me finish my research, polished my skills, and shaped my work ethics. This endeavour would not have been possible without the SLAB scholarship (UMS), Fundamental Research Grant Scheme (FRGS/1/2017/SKK12/USM/02/1), and International Program Associate (IPA) program for research funding and the opportunity to do my research in RIKEN. Special thanks to Futamura team members; Dr. Kai Yamamoto, Dr. Rachael Uson-Lopez, Dr. Sun Xiaoying, Ms. Keiko Watanabe, and Mr. Hiroyuki Uno for the technical support and friendships. I would like to thank research collaborators; Dr. Nobumoto Watanabe, Dr. Takayuki Motoyama, Dr. Shunji Takahashi, Dr. Islam A. Abdelhakim, Ms. Harumi Aono (CBRG, RIKEN), and Ms. Dayang Nurazierah Fachyuni Abdul Aziz (FSSA, UMS) for providing research materials and technical support. Special thanks to all current and past CBRG members and IPA moderators, especially Dr. Hiroyuki Hirano, Dr. Nogawa Toshihiko, Dr. Julius Adam Lopez, Dr. Mira syahfrien Amir Rawa, Ms. Okano Akiko, Ms. Satoko Yasuda, Ms. Junko Abe, Prof. K. Sudesh Kumar, and Ms. Maya Kobayashi, for their generous support in my research and daily activities. I would like to thank Mr. Atsushi Oike and his family for their continuous support, especially during the COVID-19 pandemic in Japan. Last but not least, without the endless prayers, love, support, and encouragement from my family, it would have been impossible for me to finish my research. I dedicate this thesis, especially to my loving parents, Mr. Mahmud Hussin and Mdm. Masra Nimung.

TABLE OF CONTENTS

ACKNOWLEDGEMENT	ii
TABLE OF CONTENTS.....	iii
LIST OF TABLES	xi
LIST OF FIGURES	xv
LIST OF SCHEMATIC DIAGRAMS	xxvi
LIST OF FORMULAS	xxviii
LIST OF SYMBOLS.....	xxix
LIST OF ABBREVIATIONS.....	xxx
LIST OF APPENDICES.....	xxxiii
ABSTRAK.....	xxxiv
ABSTRACT	xxxvii
CHAPTER 1 INTRODUCTION	1
1.1 Malaria: a brief background	1
1.2 Problem statement.....	2
1.2.1 Drug resistant development	2
1.2.2 Low antimalarial drug diversity.....	3
1.2.3 Antimalarials with unknown MoA	4
1.3 Strategies to solve malaria-associated problem	5
1.3.1 Drug discovery from nature	5
1.3.2 Targeting host enzymes	7
1.3.3 Targeting essential cell components for <i>Plasmodium</i> survival....	8
1.4 The rationale of the study.....	9

1.4.1	Soil actinomycetes, an inexhaustible source for bioactive compounds	9
1.4.2	<i>Hs</i> GSK-3 β inhibitor may lead to identifying new antimalarial compounds, a target-based approach	11
1.4.3	Spontaneous drug resistance development, an effective strategy to identify the antimalarial molecular target	12
1.5	Research objectives	14
1.5.1	General objective	14
1.5.2	Specific objectives	14
CHAPTER 2 LITERATURE REVIEW.....		15
2.1	Brief historical data on malaria	15
2.2	<i>Plasmodium</i> and its life cycle	19
2.3	Druggable stage of <i>Plasmodium</i> life cycle.....	21
2.4	Malaria: an ongoing battle	24
2.5	The rise of super malaria.....	30
2.6	Magic bullet and polypharmacology: Fundamental concepts in drug discovery to counter the rise of drug-resistant <i>Plasmodium</i> strain	33
2.7	Protein kinase as an emerging target to achieve magic bullet and polypharmacology.....	36
2.8	<i>Pf</i> GSK-3 inhibitors.....	45
2.9	<i>In vivo</i> yeast-based assay expressing <i>Hs</i> GSK-3 β : a target-based assay towards the identification of antimalarial compounds, possibly targeting <i>Pf</i> GSK-3	48
CHAPTER 3 MATERIAL AND METHODS.....		52
3.1	Overall methodologies	52

3.2	Bioassays.....	55
3.2.1	Yeast-based assay expressing <i>Hs</i> GSK-3 β	55
3.2.2	Antimalarial assay against <i>P. falciparum</i>	55
3.2.2(a)	RPMI[-]/[+] and bovine serum albumin (BSA) stock solution to culture <i>P. falciparum</i> and to perform the antimalarial assay	55
3.2.2(b)	Blood sample preparation	56
3.2.2(c)	Reviving <i>Pf</i> from glycerol stock	58
3.2.2(d)	Calculation of infection rate (IR)	59
3.2.2(e)	Phenotypic screening	60
3.2.2(f)	<i>Plasmodium</i> Lactate Dehydrogenase assay	61
3.2.2(g)	Threshold to determine antimalarial potency.....	62
3.3	Growth optimization of selected soil microbial strains.....	64
3.4	Extraction and heat stability tests.....	67
3.4.1	Extraction test	67
3.4.2	Heat stability test.....	69
3.5	Fractionation and purification of active compounds.....	71
3.5.1	Large scale liquid-liquid extraction (LLE)	71
3.5.2	Thin-layer chromatography (TLC)	72
3.5.3	Open column chromatography (CC) – Silica gel.....	72
3.5.4	Centrifugal Partition Chromatography (CPC)	72
3.5.5	High-performance liquid chromatography (HPLC).....	75
3.6	Structural elucidation of active compounds.....	76
3.6.1	Ultra-Performance Liquid Chromatography-Mass Spectrometry (UPLC-MS).....	76

3.6.2	High-Resolution Electrospray Ionization Time-of-Flight Mass Spectrometry (HR-ESITOF-MS).....	77
3.6.3	Nuclear Magnetic Resonance (NMR).....	77
3.7	Red blood cell (RBC) stage-specific activity.....	78
3.7.1	Sorbitol synchronization	78
3.7.2	Life-cycle timing determination.....	79
3.7.3	Drug exposure and washout targeting specific stage	82
3.8	Antimalarial MoA determination.....	83
3.8.1	Drug exposure to induce spontaneous drug resistance	83
3.8.1(a)	Continuous drug exposure	83
3.8.1(b)	Limiting dilution assay.....	85
3.8.1(c)	Total genomic extraction and purity evaluation.....	89
3.8.1(d)	Polymerase Chain Reaction of mutated genes.....	92
3.8.1(e)	Single nucleotide polymorphism (SNP) confirmation by sequencing.....	93
3.8.2	Iron-chelating assay	94
3.8.3	<i>In silico</i> study.....	95
3.9	Structure-Activity Relationship (SAR) study	96
3.10	Statistical analysis	97
	CHAPTER 4 RESULTS	98
4.1	Yeast-strain expressing <i>Hs</i> GSK-3 β : a potential preliminary assay for antimalarial drug discovery.....	98
4.2	Reproducibility antimalarial assay of samples deposited in RIKEN microbial and chemical libraries	99
4.3	Growth optimization of selected strains for mass production.....	103

4.3.1	<i>Streptomyces</i> sp. H11809.....	103
	4.3.1(a) Growth curve-optimization approach	103
	4.3.1(b) Response surface methodology (RSM)-optimization approach	104
	4.3.1(c) Growth curve- vs RSM-optimization approaches..	107
4.3.2	MI4701	108
4.3.3	RK17-A0507 and RK17-A0707	109
4.4	Extraction and heat stability tests.....	110
4.5	Purification and identification of antimalarial compounds from selected microbial extracts	112
4.5.1	<i>Streptomyces</i> sp. H11809.....	112
	4.5.1(a) Dibutyl phthalates	112
	4.5.1(b) Nocardamine	119
4.5.2	MI4701	122
	4.5.2(a) Nataxazole.....	122
4.5.3	<i>Aspergillus</i> sp. Man15558.....	127
	4.5.3(a) Secalonic acid derivatives.....	127
4.5.4	RK17-A0610 and RK18-A0619	134
	4.5.4(a) Nocardamine	134
4.5.5	RK17-A0507.....	135
4.5.6	RK17-A0707	141
4.5.7	Overall identified compounds	154
4.6	Mode of actions (MoA).....	155
4.6.1	Dibutyl phthalates: GSK-3 inhibitor	155

4.6.1(a)	The molecular target of DBP might be essential for <i>Plasmodium</i> survival.....	155
4.6.1(b)	DBP showed selective inhibitory against <i>Hs</i> GSK-3 β <i>in vivo</i>	156
4.6.1(c)	DBP binds on <i>Hs</i> GSK-3 β Arg96, a conserved amino acid in <i>Pf</i> GSK-3	157
4.6.2	Nataxazole and secalonic acid potentially targeting human and <i>Plasmodium</i> GSK-3	159
4.6.3	Nocardamine starves <i>Plasmodium</i> from its iron source.....	161
4.6.4	CP31178 disrupt heme degradation by <i>Plasmodium</i>	163
4.6.4(a)	<i>Pf</i> 3D7 IC ₅₀ of CP31178	163
4.6.4(b)	Successful generation of CP31178 resistant clone	164
4.6.4(c)	CP31178 exerts similar MoA as CQ.....	165
4.6.5	Dihydrolucilactaene (DHLC): an ultrapotent antimalarial with novel molecular target.....	167
4.6.5(a)	<i>Pf</i> 3D7 IC ₅₀ of DHLC	167
4.6.5(b)	DHLC is mainly targeting the trophozoites during the <i>Plasmodium</i> RBC life cycle	168
4.6.5(c)	DHLC slows down <i>P. falciparum</i> egression during the RBC stage	170
4.6.5(d)	DHLC exerts a different MoA than ART and CQ, but maybe similar with ATO.....	174
4.6.5(e)	Successful generation of DHLC-resistant strain via continuous drug-exposure	175

4.6.5(f)	Limiting dilution assay of <i>Pf</i> DHLC-4 to select a single mutant clone	176
4.6.5(g)	Genome sequencing from <i>Pf</i> DHLC-4 W1 and W4 to identify DHLC plausible molecular target.....	180
4.6.5(h)	Single nucleotide polymorphism confirmed gene #6 as the mutated gene induced by DHLC.....	182
4.6.5(i)	Successful re-generation of DHLC resistance clone with a similar mutation on gene #6.....	185
4.6.5(j)	DHLC has different MoA than ATO	189
4.7	Structure-Activity Relationship (SAR) of lucilactaene derivatives	190
CHAPTER 5 DISCUSSION		195
5.1	Soil microorganisms as an exciting source for antimalarials.....	195
5.2	The potential of the target-based assay against <i>Hs</i> GSK-3 β in antimalarial drug discovery targeting <i>Pf</i> GSK-3: An approach to achieve magic bullet and polypharmacology	202
5.3	Nocardamine: Starves <i>Plasmodium</i> from its iron source under <i>in vitro</i> setting	208
5.4	Successful generation of CP31178-resistant <i>Plasmodium</i> strain: Towards uncovering the mode of action of methylene blue and its derivatives...	210
5.5	Dihydrolucilactaene: A new prime candidate for future antimalarials with a novel mode of action	213
5.6	Outlook: Overall therapeutic potential beyond the <i>P. falciparum</i> infection treatment.....	215
5.6.1	Antimalarial activity against <i>P. vivax</i> and <i>P. knowlesi</i> : The implications.....	215

5.6.2	<i>Hs</i> GSK-3 β inhibitor: Potential therapeutic uses across diverse diseases for future drug repurposing.....	218
5.6.3	One strain many active compounds (OSMAC) approach to identify potential potent antimicrobial activity	220
CHAPTER 6	CONCLUSION.....	222
6.1	Overall conclusion	222
6.2	Limitation of the study	224
6.3	Future recommendations	225
REFERENCES		227
APPENDICES		
LIST OF PUBLICATIONS		

LIST OF TABLES

	Page
Table 2.1	Classes of antimalarial agents, their members, structures, MoA and current status25
Table 2.2	List of <i>Plasmodium falciparum</i> eukaryotic protein kinase37
Table 2.3	Identity (exact match) dan similarity (resemblance) index of GSK-3 between human and <i>Plasmodium</i> parasites.....41
Table 2.4	The interpretation of results based on the possible zone of inhibition patterns51
Table 3.1	pLDH reaction mix for 96-well plate (150 μ L/well or 15 mL/96-well plate61
Table 3.2	The morphologies and bioactivities of selected potent strains..... 66
Table 3.3	Flasks/runs and their parameters to conduct RSM of <i>Streptomyces</i> sp. H1180967
Table 3.4	The methodologies to run CPC analysis74
Table 3.5	The details of primers used in this study92
Table 3.6	The PCR cocktails.....93
Table 3.7	The optimized parameters to perform PCR of the possibly mutated genes93
Table 3.8	The mixture for PCR product sequencing94
Table 4.1	Bioactivities of strains isolated from Malaysia.....100
Table 4.2	Bioactivities of the crude extracts of Japanese strains and pure compounds deposited at RIKEN chemical library.....101

Table 4.3	The <i>Hs</i> GSK-3 β inhibitory activity of <i>Streptomyces</i> sp. H11809 crude extracts from day 1-10 incubation period103
Table 4.4	The ANOVA analysis of RSM to develop a model to predict the production of overall secondary metabolites105
Table 4.5	The analysis of R-squared.....105
Table 4.6	Experiment to validate the acquired model equation.....106
Table 4.7	The comparison between growth curved-optimized and RSM-optimized conditions regarding the amount of secondary metabolites production (g/L) and inhibitory activity against <i>Hs</i> GSK-3 β107
Table 4.8	The <i>Hs</i> GSK-3 β inhibitory activity of MI4701 crude extracts from day 1-10 incubation period108
Table 4.9	Extraction and heat stability tests of selected strains.....110
Table 4.10	The inhibitory activity of H11809-CHCl ₃ CC fractions against <i>Hs</i> GSK-3 β112
Table 4.11	The comparison of ¹ H-NMR of H11809-CCF8 and reported NMR analysis of DBP.....115
Table 4.12	The comparison of ¹³ C-NMR of H11809-CCF8 and reported NMR analysis of DBP.....116
Table 4.13	¹ H-NMR spectral data comparison of nataxazole from previously reported (1) (Sommer et al., 2008) and this study (2).....124
Table 4.14	Bioactivities of Man-Hex and Man-CHCl ₃126
Table 4.15	Antimalarial activity of Man15558-hexane HPLC fractions.....127
Table 4.16	Unidentified secalonic acid derivatives. These derivatives have similar [M+H] ⁺ <i>m/z</i> and chemical formula as secalonic acid F, but

	different UV signal and RT, indicating the presence of different derivatives of secalonic acid	131
Table 4.17	LCMS analysis of HPLC fractions collected from A0507 EA CPC-RF1 (fraction 33, F33) and A0507 EA CPC-RF5 (fraction 34, F34)	137
Table 4.18	The cytotoxic, antimicrobial, and antifungal activities of active compounds purified from RK17-A0507	138
Table 4.19	The antimalarial activities of the CPC fractions of A0707 EA	141
Table 4.20	The antimalarial activity of A0707 EA 2 nd CPC-NF1	142
Table 4.21	The antimalarial activity of A0707 EA 3 rd CPC fractions	143
Table 4.22	IC ₅₀ determination of A0707 EA 3 rd CPC-NF2-M and A0707 EA 3 rd CPC-NF2-C. A0707 EA 3 rd CPC-NF2-C showed more potent activity than A0707 EA 3 rd CPC-NF2-M. However, these fractions showed similar IC ₅₀ against mutant strain, <i>Pf</i> 1-1-C07	145
Table 4.23	The fraction collection time of A0707 EA 3 rd CPC-NF2-C and the amount of the respective fraction.....	146
Table 4.24	Antimalarial activity of A0707 EA 3 rd CPC-NF2-C fractions.....	147
Table 4.25	The overall compounds identified/suggested in this study	153
Table 4.26	The activity of DBP and nocardamine against <i>Hs</i> GSK-3 β	156
Table 4.27	The effect of iron supplement on the antimalarial effect of nocardamine	161
Table 4.28	Morphological changes induced by DHLC during the RBC stage of synchronized <i>Pf</i> culture. DHLC was applied-washed at a specific time to target ring, trophozoites, and schizont stages	172

Table 4.29	Morphological changes induced by CQ during RBC stage of synchronized <i>Pf</i> culture. CQ was applied-washed at a specific time to target ring, trophozoites, and schizont stages	173
Table 4.30	The IC ₅₀ of DHLC against <i>Pf</i> 3D7 and exposed strains, to determine resistant development.....	176
Table 4.31	Plausible mutated genes from <i>Pf</i> DHLC-4 W1 and <i>Pf</i> DHCL-4 W4 as identified from whole-whole genome sequencing.....	181
Table 4.32	Overall occurrence of SNP of identified mutated genes, validated by sequencing of PCR product	182
Table 4.33	The IC ₅₀ of DHLC against generated strain from batch 2. <i>Pf</i> 2-DHLC-4 developed the most significant resistant phenotype	186
Table 4.34	The resistance development of strains selected from DHLC-exposure (batch-2).....	188
Table 4.35	The IC ₅₀ of lucilactaene derivatives.....	191
Table 4.36	The IC ₅₀ values comparison of lucilactaene derivatives, analyzed using ANOVA at a 99 % confidence level	192
Table 4.37	The statistical analysis of lucilactaene derivatives in this study was analyzed using ANOVA at a 99 % confidence level.....	193

LIST OF FIGURES

	Page
Figure 2.1	The life cycle of <i>P. falciparum</i> (Matthews et al., 2018). Created with BioRender.com 21
Figure 2.2	Essential protein kinase required for <i>P. falciparum</i> survival at a different stage of its life cycle. Created with BioRender.com... 40
Figure 2.3	The ATP binding site of GSK-3. Gatekeeper residue (R) is guarding the hydrophobic pocket. The size of the ATP gatekeeper is one of the possible structural features that can be exploited to achieve selectivity (Turner, 2020) 43
Figure 2.4	Binding interaction of thienopyridine analog with mammalian GSK-3 (top). The docking of 3,6-Diamino-4-(2-halophenyl)-2-benzoylthieno [2,3-b]pyridine-5-carbonitriles with the homology model of GSK-3 (bottom) (Fugel et al., 2013; Turner, 2020) .. 47
Figure 3.1	Concentrated blood sample (type A) obtained from the Japanese Red Cross society (left). The blood was centrifuged to remove access blood serum—a clear upper layer indicating low-fat contents, suitable for <i>P. falciparum</i> culture (right)..... 57
Figure 3.2	The area to calculate infected (yellow + orange) and non-infected (yellow) RBC cells..... 60
Figure 3.3	Overall experimental procedure to perform the antimalarial assay. Created with BioRender.com..... 63
Figure 3.4	Experimental design to perform extraction and heat stability tests. Created with BioRender.com..... 70

Figure 3.5	Synchronization of <i>Pf</i> culture using sorbitol. <i>Pf</i> culture with most ring stage was selected for sorbitol treatment 1 (denoted as <i>Pf</i> sorbitol 1) and incubated for 48 h (a). A large amount of ring was observed after <i>Pf</i> sorbitol 1. The culture was treated for sorbitol treatment 2 (<i>Pf</i> sorbitol 2). After 48 h, the culture was then treated with third sorbitol (<i>Pf</i> sorbitol 3) (b). 32 h after <i>Pf</i> sorbitol 3, <i>Pf</i> growth was observed under the microscope by which many trophozoites were observed. It indicates the culture is ready for antimalarial assay. The culture was culture for another 16 h (c). Before the screening, the fourth sorbitol treatment (<i>Pf</i> sorbitol 4) was performed. Only the ring stage was observed (d)..... 81
Figure 3.6	The established life cycle of <i>Pf</i> 3D7 used in this study (42 h)... 82
Figure 3.7	Experimental design to determine the stage-specific activity of the test compounds. Created with BioRender.com..... 83
Figure 3.8	Experimental design to induce spontaneous mutation-bearing drug resistance phenotype by continuous drug exposure. This process mimics the actual drug-resistance development in nature. Created with BioRender.com 85
Figure 3.9	General method to perform limiting dilution assay, to select a single clone to be scaled up for a further test and genomic extraction for whole-genome sequencing. Created with BioRender.com 88
Figure 3.10	The 1 kb ladder (Biolabs) used to estimate the size of DNA bands 91
Figure 3.11	Lucilactaene derivatives tested to establish the SAR..... 97

Figure 4.1	The growth curve of <i>Streptomyces</i> sp. H11809	103
Figure 4.2	The 3-D (left) and contour (right) graphs, to visualize a significant optimized model (p-value <0.0001).....	105
Figure 4.3	The growth curve of MI4701	108
Figure 4.4	Daily antimalarial activity of RK17-A0507 and RK17-A0707 cultured in 2L baffled and non-baffled flasks.....	109
Figure 4.5	The TLC profile of H11809-CHCl ₃ CC fractions (60 fractions) viewed at 365 nm, pooled into 9 fractions.....	111
Figure 4.6	The MS analysis of H11809-CCF8.....	113
Figure 4.7	Retention time (RT) comparison of commercially available DBP and active compound in H11809-CCF8.....	114
Figure 4.8	¹ H-NMR spectrum of H11809-CCF8	115
Figure 4.9	The ¹³ C-NMR spectrum of H11809-CCF8	116
Figure 4.10	<i>Pf</i> 3D7 IC ₅₀ determination of DBP (Log IC ₅₀ = 0.6 µg/mL, IC ₅₀ = 4.0 µg/mL or 14.4 µM, and R ² = 0.9)	117
Figure 4.11	MS analysis of HPLC-CCF9.....	118
Figure 4.12	Retention time (RT) comparison of commercially available nocardamine and active compound in H11809-CCF9.....	119
Figure 4.13	<i>Pf</i> 3D7 IC ₅₀ determination of nocardamine (Log IC ₅₀ = 0.2 µM, IC ₅₀ = 1.5 µM, and R ² = 0.9).....	119
Figure 4.14	MS analysis of MI4701 EA-RF3-F42.....	122
Figure 4.15	The HR-ESITOF-MS analysis of MI4701 EA-RF3-F42 indicated nataxazole as the plausible active compound	122
Figure 4.16	<i>Pf</i> 3D7 IC ₅₀ determination of nataxazole (Log IC ₅₀ = 0.8 µg/mL, IC ₅₀ = 5.9 µg/mL or 14.7 µM, and R ² = 0.9).....	124

Figure 4.17	Mass chromatogram of Man-Hex F8. Major peak at RT ~3.4 minutes (with $[M+H]^+$ 639.5 m/z) was identified 128
Figure 4.18	HR-ESITOF-MS analysis of Man-Hex F8 128
Figure 4.19	Secalonic acid F standard and Man-Hex F8 showed similar RT (left) and similar UV profiles (right). UV profile of commercial secalonic acid F (a) and Man-Hex F8 (b) 129
Figure 4.20	<i>Pf</i> 3D7 IC_{50} determination of secalonic acid F (Log IC_{50} = 0.6 μ M, IC_{50} = 4.1 μ M, and R^2 = 0.9)..... 130
Figure 4.21	The RT of nocardamine (red line) and active compounds in UMS and RIKEN samples..... 133
Figure 4.22	CPC fractionation of A0507 EA by which A0507 EA CPC-RF1 and A0507 EA CPC-RF5 were identified with potent (+++) antimalarial activity..... 135
Figure 4.23	The colors of purified compound from A0707 EA CPC-RF1-F33 (red) (a) and -F34 (yellow) (b) and plausible active compounds. A0707 EA CPC-RF1-F33 was suggested as hibarimicin C and no exact match on DNP for A0707 EA CPC-RF5-F34 136
Figure 4.24	<i>Pf</i> 3D7 IC_{50} determination of A0707 EA CPC-RF1-F33 (Log IC_{50} = -1.4 μ g/mL, IC_{50} = 0.04 μ g/mL, and R^2 = 0.9) and A0707 EA CPC-RF5-F34 (Log IC_{50} = -1.5 μ g/mL, IC_{50} = 0.03 μ g/mL, and R^2 = 0.9) 137
Figure 4.25	CPC fractionation of A0707 EA 141
Figure 4.26	<i>Pf</i> 1-1-C07, clone strain expressing mutant <i>Pf</i> ATP4 significantly has reduced sensitivity towards RK17-A707 RF10 (6000-fold)

	compared to the WT <i>Pf</i> 3D7, which indicates the presence of antimalarial agent(s) targeting <i>Pf</i> ATP4 as its possible MoA..	142
Figure 4.27	CPC fractionation of A0707 EA 1 st CPC-RF10.....	142
Figure 4.28	CPC fractionation of A0707 EA 2 nd CPC-NF1	143
Figure 4.29	The phenotypic observation of A0707 EA 3 rd CPC-NF2-M and EA 3 rd CPC-NF2-C against <i>Pf</i> 3D7 and <i>Pf</i> 1-1C07	145
Figure 4.30	HPLC analysis of A0707 EA 3 rd CPC-NF2-C (1.0 mg). The chromatogram was viewed at 200 nm.....	146
Figure 4.31	The phenotypic observation of A0707 EA 3 rd CPC-NF2-C HPLC fractions against <i>Pf</i> 3D7	147
Figure 4.32	<i>Pf</i> 3D7 IC ₅₀ determination of A0707 EA 3 rd CPC-NF2-C P8 (Log IC ₅₀ = -2.058 µg/mL, IC ₅₀ = 0.009 µg/mL, and R ² = 0.9); a highly potent antimalarial.....	148
Figure 4.33	LCMS analysis of purified compounds. A0707 EA 3 rd CPC-NF2-C P5 (-), A0707 EA 3 rd CPC-NF2-C P8 (++++), and A0707 EA 3 rd CPC-NF2-C P11 (++) were viewed at 200 nm. The peak at ~RT 2.3 min is not the active compound. Meanwhile, peaks at ~RT 3.7 min (main interests, potent compound) and ~RT 4.5 min are possibly other active compounds with moderate activity	149
Figure 4.34	The MS data of A0707-EA 3 rd CPC-NF2-C P8.....	150
Figure 4.35	The MS/MS data obtained from HR-ESITOF-MS. The mass in the circle is the common fragmentation observed in the reported MS/MS data of koranimine.....	151
Figure 4.36	The method was applied to generate a DBP-resistant <i>Pf</i> strains (left). The IC ₅₀ comparison of DBP against <i>Pf</i> 3D7 (Log IC ₅₀ = 0.6	

	$\mu\text{g/mL}$, $\text{IC}_{50} = 4.0 \mu\text{g/mL}$ or $14.4 \mu\text{M}$, and $R^2 = 0.9$) and <i>Pf</i> DBP-4 ($\text{Log IC}_{50} = 0.8 \mu\text{g/mL}$, $\text{IC}_{50} = 6.2 \mu\text{g/mL}$ or $22.3 \mu\text{M}$, and $R^2 = 0.9$)	155
Figure 4.37	The observation of DBP and nocardamine against <i>Hs</i> GSK-3 β activity <i>in vivo</i> . DBP exerted selective <i>Hs</i> GSK-3 β inhibition (a)	155
Figure 4.38	Two-dimensional Ligplot ⁺ diagram of the interaction between DBP and amino acid residues on the ATP-binding site (P1) (binding affinity = -6.1 kcal/mol) (left) and substrate-binding site (P2) (binding affinity = -6.9 kcal/mol) (right) of <i>Hs</i> GSK-3 β . No hydrogen bond was formed in P1 by DBP. Meanwhile, DBP formed two hydrogen bonds with Arg96 and Glu97. Green dashed lines = hydrogen bonds, red spoked arcs = hydrophobic interaction, red dots = oxygen, blue dots = nitrogen and grey dots = carbon.....	157
Figure 4.39	Two-dimensional Ligplot ⁺ diagram of the interaction between nataxazole and amino acid residues on the ATP-binding site (P1) (left) and substrate-binding site (P2) (right) of <i>Hs</i> GSK-3 β . One hydrogen bond was formed in P1 by nataxazole (Lys85) (binding affinity = -10.5 kcal/mol). Meanwhile, five hydrogen bonds were formed by nataxazole in P2 (Lys292 and Arg96) (binding affinity = -8.1 kcal/mol).....	159
Figure 4.40	Two-dimensional Ligplot ⁺ diagram of the interaction between secalonic acid F and amino acid residues on the ATP-binding site (P1) (left) and substrate-binding site (P2) (right) of <i>Hs</i> GSK-3 β . A	

	total of three hydrogen bonds were formed in P1 by secalonic acid F (Tyr134, Asp200, Asn186) (binding affinity = -8.8 kcal/mol). Meanwhile, two hydrogen bonds were formed by secalonic acid F in P2 (Lys205) (binding affinity = -6.4 kcal/mol)	160
Figure 4.41	Suggested antimalarial MoA of nocardamine. The addition of $\geq 12.5 \mu\text{M Fe}^{3+}$ reduced the efficiency of nocardamine by 90 % against <i>Pf</i> 3D7, indicating <i>Pf</i> iron starvation as the antimalarial MoA of nocardamine	162
Figure 4.42	IC ₅₀ determination of CP31178 (Log IC ₅₀ = -1.6 μM , IC ₅₀ = 0.02 μM , and R ² = 0.9). Red dots represent cytotoxic activity of CP31178 against <i>Pf</i> 3D7 at high concentration	162
Figure 4.43	pLDH assay to determine the effect of CP31178 on WT and CP31178-exposed strains (top). The activity of CPC31178 against <i>Pf</i> 3D7 (WT) and possible mutant clones, <i>Pf</i> CP-04 and CP-05. Parasite clearance of <i>Pf</i> 3D7, <i>Pf</i> CP-04 (mutant), and <i>Pf</i> CP-05 (mutant) against CP31178 (bottom). Both <i>Pf</i> CP-04 and <i>Pf</i> CP-05 developed resistance phenotype against CP31178.....	164
Figure 4.44	Parasite clearance of <i>Pf</i> 3D7, <i>Pf</i> CP-04 (mutant), and <i>Pf</i> CP-05 (mutant) against CQ (positive control). Both <i>Pf</i> CP-04 and <i>Pf</i> CP-05 developed resistance phenotype against CQ.....	165
Figure 4.45	<i>Pf</i> 3D7 IC ₅₀ determination of CP31178 against <i>Pf</i> 3D7 (WT) and <i>Pf</i> K1 (CQ-resistant). CP31178 <i>Pf</i> 3D7 IC ₅₀ = 0.01 μM , and <i>Pf</i> K1 IC ₅₀ = 0.07 μM (7-fold).....	166

Figure 4.46	The morphology of <i>Fusarium</i> sp. 97-94 under the microscope (left). The structure of DHLC, a new lucilactaene derivative that showed highly potent antimalarial activity (right)..... 166
Figure 4.47	IC ₅₀ determination of DHLC against <i>Pf</i> 3D7 (Log IC ₅₀ = 0.1 nM, IC ₅₀ = 1.4 nM, and R ² = 0.9)..... 167
Figure 4.48	The effect of CQ (top) and DHLC (below) on sorbitol-synchronized <i>Pf</i> culture, tested at IC ₉₀ , IC ₅₀ , and IC ₂₀ 168
Figure 4.49	pLDH assay to determine the effect of DHLC different stage of <i>Pf</i> (RBC stage) (top). Stage-specific IC ₅₀ determination of DHLC against <i>Pf</i> 3D7 (Ring-Log IC ₅₀ = 0.9 nM, IC ₅₀ = 8.2 nM, and R ² = 0.8; trophozoites-Log IC ₅₀ = -0.2 nM, IC ₅₀ = 0.6 nM, and R ² = 1.0; schizont- Log IC ₅₀ = 0.5 nM, IC ₅₀ = 3.5 nM, and R ² = 0.9; non-synchronized (60 h)- Log IC ₅₀ = -1.1 nM, IC ₅₀ = 0.1 nM, and R ² = 1.0) (bottom) 169
Figure 4.50	IC ₅₀ determination of DHLC against <i>Pf</i> 3D7 and <i>Pf</i> K1. DHLC exerted similar IC ₅₀ (<i>Pf</i> 3D7 IC ₅₀ - Log IC ₅₀ = 0.1 nM, IC ₅₀ = 1.4 nM, and R ² = 1.0; <i>Pf</i> K1 IC ₅₀ - Log IC ₅₀ = 0.1 nM, IC ₅₀ = 1.4 nM, and R ² = 0.9) against both strains (right). Meanwhile, <i>Pf</i> K1 is ~8-fold more resistant towards CQ than <i>Pf</i> 3D7 (WT), indicating DHLC and CQ has different MoA (<i>Pf</i> 3D7 IC ₅₀ - Log IC ₅₀ = 1.0 nM, IC ₅₀ = 8.6 nM, and R ² = 1.0; <i>Pf</i> K1 IC ₅₀ - Log IC ₅₀ = 1.5 nM, IC ₅₀ = 29.7 nM, and R ² = 1.0 (left) 171
Figure 4.51	The comparison of DHLC and prolific antimalarials (ART, CQ, ATO) RBC stage-specific profile 175

Figure 4.52	pLDH analysis of limiting dilution plate to identify well with <i>Pf</i> growth, to be upscaled. W1, W4, W7 and W8 were selected for upscale culture..... 177
Figure 4.53	The activity of DHLC against <i>Pf</i> 3D7 vs. <i>Pf</i> DHLC-4 W4. The OD of <i>Pf</i> 3D7 (IR=0.3 %) in the presence of DMSO is 1.049 (not affected by DMSO. Hence inhibitory effect observed is from DHLC), which is comparable to <i>Pf</i> DHLC-4 W4 (IR=0.6 %), with an OD of 1.089. Meanwhile, the OD of <i>Pf</i> DHLC-4 W4 (IR=0.3 %) in the presence of DMSO is 0.638, indicating inhibitory activity observed was due to effect of both DHLC and DMSO 178
Figure 4.54	The IC ₅₀ values of DHLC on <i>Pf</i> 3D7 (WT) vs. four different clones of <i>Pf</i> DHLC-4 selected from the limiting dilution experiment (denoted as W1, W4, W7, and W8; W = well) on week 4. <i>Pf</i> 3D7 IC ₅₀ - Log IC ₅₀ = 0.1 nM, IC ₅₀ = 1.4 nM, and R ² = 1.0; <i>Pf</i> DHLC-4 W1 IC ₅₀ - Log IC ₅₀ = 1.3 nM, IC ₅₀ = 19.5 nM, and R ² = 1.0; <i>Pf</i> DHLC-4 W4 IC ₅₀ - Log IC ₅₀ = 1.4 nM, IC ₅₀ = 24.4 nM, and R ² = 1.0; <i>Pf</i> DHLC-4 W7 IC ₅₀ - Log IC ₅₀ = 1.0 nM, IC ₅₀ = 9.9 nM, and R ² = 1.0; <i>Pf</i> DHLC-4 W8 IC ₅₀ - Log IC ₅₀ = 0.9 nM, IC ₅₀ = 8.4 nM, and R ² = 0.9 (left). All strains showed significant (one-way ANOVA, P-value = 0.1) DHLC-resistance phenotype compared to WT, but <i>Pf</i> DHLC-4 W1 and <i>Pf</i> DHLC-4 W1 had retained a similar observation after 4 weeks. One-way ANOVA (p-value = 0.1) (right) 179

Figure 4.55	Gel electrophoresis of total genomic DNA obtained from <i>Pf</i> 3D7 (WT) and two DHLC-resistance clones (<i>Pf</i> DHLC-4 W1 and W4). High-quality genomic DNA was obtained for total genome sequencing..... 180
Figure 4.56	The agarose gel electrophoresis of DHLC-4 W4 PCR product and its respective OD ratio at A260/280. A high-quality PCR product was obtained for reliable sequencing 182
Figure 4.57	Alignment of the targeted region of gene #6. WT_#6_2643fw – sequence of WT, DHLC-4_#6_2643fw – a resistant pool that displayed DHLC-resistant phenotype, DHLC-4-W1_#6_2643fw and DHLC-4-W4_#6_2643fw – single mutant clone obtained from limiting dilution assay of DHLC-4..... 183
Figure 4.58	Nucleotide chromatogram of the targeted region confirmed the nucleotide sequence (a). Amino acid translation (b)..... 184
Figure 4.59	Sequence of <i>Pf</i> DHLC-4 W4 was compared with gene #6 deposited in the NCBI database 185
Figure 4.60	The method applied to generate DHLC resistant strain for batch 1 (left) and batch 2 (right). Created with BioRender.com 186
Figure 4.61	pLDH analysis of limiting dilution plate (batch 2) to identify well with <i>Pf</i> growth, to be upscaled. Wells numbered as 1-8 were selected for upscale culture 187
Figure 4.62	The agarose gel electrophoresis of <i>Pf</i> DHLC-4 W4 PCR product and its respective OD ratio at A260/280. A high-quality PCR product was obtained for reliable sequencing (top). Alignment of the targeted region of gene #6 of strains generated in batch 1 and

batch 2. WT_#6_2643fw – sequence of WT (*Pf* 3D7), DHLC-4-W1_#6_2643fw, and DHLC-4-W1_#6_2643fw – single mutant clone obtained from batch 1. 2-DHLC-4-1, 2-DHLC-4-3, 2-DHLC-4-4, and 2-DHLC-4-7 – single mutant clone obtained from batch 2 (bottom)..... 189

Figure 4.63 The effect of DHLC (left) and ATO (right) on WT and DHLC-resistant strains; DHLC-4 W4 (form batch 1) and 2-DHLC-4 4 (from batch 2). Mutated strains are resistant towards DHLC (*Pf* 3D7 IC_{50} - $\text{Log } IC_{50} = 0.2$ nM, $IC_{50} = 1.4$ nM, and $R^2 = 1.0$ (12-fold); *Pf* DHLC-4 W4 - $\text{Log } IC_{50} = 1.3$ nM, $IC_{50} = 18.2$ nM, and $R^2 = 1.0$; *Pf* 2-DHLC-4 4 - $\text{Log } IC_{50} = 1.1$ nM, $IC_{50} = 11.5$ nM, and $R^2 = 1.0$ 8-fold))(left). Meanwhile, ATO exerted similar IC_{50} (~0.4 nM; $\text{Log } IC_{50} = -0.4$ nM, $IC_{50} = 0.4$ nM, and $R^2 = 1.0$) on all strains, indicating DHLC and ATO has different molecular target (right) 190

Figure 4.64 The influence of structural differences in lucilactaene derivatives. The opening of the tetrahydrofuran ring (green) leads to a 100-fold increase in antimalarial activity. The epoxide (yellow) removal results in a 1200-fold increase in antimalarial activity. These findings contradict than previous SAR of lucilactaene..... 191

Figure 4.65 Overall SAR of lucilactaene and its derivatives. The same highlighting color suggests the compounds are identical in overall structure except at the highlighted position. These highlighted positions are accountable for the statistically significant differences in IC_{50} values..... 193

LIST OF SCHEMATIC DIAGRAMS

	Page
Schematic diagram 3.1	The overall methodologies performed in this study..... 54
Schematic diagram 3.2	Overall methodologies to perform <i>Pf</i> sorbitol (5 %(w/v)) synchronization 79
Schematic diagram 4.1	The summary of the experiment conducted to identify active compounds from <i>Streptomyces</i> sp. H11809. DBP and nocardamine were identified as the active compounds..... 120
Schematic diagram 4.2	The summary of the experiment conducted to identify active compounds from MI4701. Nataxazole was identified as the active compound..... 125
Schematic diagram 4.3	The summary of the experiment conducted to identify active compounds from <i>Aspergillus</i> sp. Man1558. Secalonic acid F was identified as the active compound..... 132
Schematic diagram 4.4	The summary of the experiment conducted to identify active compounds from RK17-A0610 and RK18-A0619 led to the identification of nocardamine 134
Schematic diagram 4.5	The summary of the experiment conducted to identify active compounds from RK17-A0507 that lead to identifying highly potent but toxic antimalarial, hibarimicin C/hibarimicin derivatives 139

Schematic diagram 4.6 The summary of the experiment conducted to identify active compounds from RK17-A0707 that lead to identifying highly potent antimalarial, suggested as koranimine derivatives..... 152

LIST OF FORMULAS

	Page
Formula 3.1	Formula to calculate <i>Pf</i> IR to perform <i>Pf</i> passing and assay 60
Formula 3.2	The formula to calculate the IR of <i>Pf</i> 3D7 (pLDH assay) 62
Formula 3.3	The formula to calculate the amount of parasite/ μ L, proposed by World Health Organization (WHO). On average, there are around 5 million RBC/ μ L 86
Formula 4.1	A model equation to predict the amount of metabolites (g/L) produced by <i>Streptomyces</i> sp. H11809 104

LIST OF SYMBOLS

α	Alpha
\AA	Angstrom
β	Beta

LIST OF ABBREVIATIONS

ACT	Artemisinin Combination Therapy
AD	Anno Domini
AGC	PKs A, G and C
ANOVA	Analysis of Variance
ART	Artemisinin
ATO	Atovaquone
ATP	Adenosine triphosphate
BC	Before Christ
BSA	Bovine serum albumin
CaMK	Calmodulin-dependent protein kinase
CBRG	Chemical Biology Research Group
CC	Column chromatography
CCD	Central Composite Design
CK1	Casein kinase 1
CMGC	CDK, MAPK, GSK3, CK2
CPC	Centrifugal Partition Chromatography
CQ	Chloroquine
DBP	Dibutyl phthalates
DHLC	Dihydrolucilactaene
DMSO	Dimethyl sulfoxide
DNA	Deoxyribonucleic acid
DV	Digestive vacuole
EE	Exoerythrocytic schizogony

eIF2	Eukaryotic initiation factor 2
ePK	Eukaryotes protein kinase
FDA	Food and Drug Administration
FIKK	Phe-Ile-Lys-Lys motif
FSSA	Fakulti Sains dan Sumber Alam
GSK-3	Glycogen Synthase Kinase-3
HPLC	High-performance Liquid Chromatography
HR-ESITOF-MS	High-Resolution electro ionization time-of-flight mass spectrometry
<i>Hs</i>	<i>Homo sapiens</i>
iHOPE	in-house-Phenotypic-Evaluation
INFORMM	Institute for Research in Molecular Medicine
IR	Infection rate
LLE	Liquid-liquid extraction
MoA	Mode of action
NMA	Never in mitosis gene
NMR	Nuclear magnetic resonance
OB	Oatmeal broth
OD	Optical density
<i>Pb</i>	<i>Plasmodium berghei</i>
PCR	Polymerase chain reaction
PE	Pre-erythrocytic cycle
<i>Pf</i>	<i>Plasmodium falciparum</i>
<i>Pf</i> PK	<i>Plasmodium falciparum</i> protein kinase

pLDH	<i>Plasmodium</i> lactate dehydrogenase
PV	Parasitophorous vacuole
RBC	Red blood cells
RIKEN	Rikagaku Kenkyusho
RSM	Response surface methodology
SAR	Structure-Activity Relationship
SEA	Southeast Asia
SNP	Single nucleotide polymorphism
STE	“Sterile-phenotype” kinases
TKL	Tyrosine kinase-like kinases
TLC	Thin-layer chromatography
UKM	Universiti Kebangsaan Malaysia
UMS	Universiti Malaysia Sabah
UPLC-MS	Ultra-performance Liquid Chromatography-Mass Spectrometry
USM	Universiti Sains Malaysia
WHO	World Health Organization
ZOI	Zone of inhibition

LIST OF APPENDICES

- Appendix A Chemicals to prepare mannitol-peptone broth and SC -Ura
- Appendix B Chemicals to prepare media to optimize RIKEN strains

PENGENALPASTIAN SEBATIAN ANTIMALARIA DAN MOD TINDAKANNYA

ABSTRAK

Malaria merupakan salah satu penyakit berjangkit yang paling signifikan di kawasan tropika yang telah menyebabkan hampir setengah juta kematian setiap tahun, terutamanya disebabkan oleh jangkitan *Plasmodium falciparum* (*P. falciparum*). Sehingga kini, *P. falciparum* telah membangunkan rintangan penuh atau separa terhadap ketiga-tiga kelas antimalaria, termasuk artemisinin. Maka, ia boleh menjejaskan keberkesanan Terapi Gabungan Artemisinin (ART) pada masa hadapan. Oleh itu, terdapat keperluan untuk mengenal pasti sebatian antimalaria dengan mod tindakan baharu. Matlamat utama kajian ini adalah untuk mengenal pasti sebatian antimalaria baharu daripada mikroorganisma tanah yang diisolasi daripada Malaysia dan Jepun. Ekstrak mentah strain-strain ini telah menunjukkan aktiviti antimalaria yang poten pada saringan awal terhadap strain *Pf* 3D7 (jenis liar). Ekstrak mentah strain daripada Malaysia juga telah merencatkan aktiviti GSK-3 β manusia (*Hs* GSK-3 β) (75 % serupa dengan GSK-3 *P. falciparum* (*Pf* GSK-3)). Maka, terdapat potensi untuk mengenal pasti sebatian antimalaria yang merencatkan aktiviti *Pf* GSK-3, iaitu mod tindakan baharu. Selain itu, tiga sebatian tulen baharu yang disimpan di

perpustakaan kimia RIKEN juga telah dinilai dalam ujian keboleholangan aktiviti antimalaria untuk memilih sebatian yang paling poten sebelum penentuan mod tindakan. Secara keseluruhannya, 18 sebatian antimalaria telah dikenal pasti/dicadangkan antaranya dibutil phthalates (DBP) ($IC_{50} = 14.4 \mu M$), nataxazole (agen antimalaria baharu, $IC_{50} = 14.7 \mu M$) dan asid sekalonik F ($IC_{50} = 4.1 \mu M$) (daripada strain Malaysia) dan hibarimisin C (agen antimalaria baharu, $IC_{50} = \sim 0.02 \mu M$) (daripada strain Jepun). Kajian *in silico* telah menunjukkan bahawa DBP, nataxazole, dan asid sekalonik F telah membentuk ikatan hidrogen dengan residu asid amino penting pada *Hs* GSK-3 β (masing-masing dengan Arg87, Lys85, dan Asp200,) yang juga terdapat pada *Pf* GSK-3 (masing-masing sebagai Arg119, Lys108, dan Asp225). Oleh itu, aktiviti antimalaria sebatian-sebatian ini berkemungkinan hasil daripada perencatan aktiviti *Pf* GSK-3. Sementara itu, dihydrolucilactaene (DHLC, sebatian baharu daripada *Fusarium* sp. 97-94 yang telah didepositkan ke perpustakaan kimia RIKEN) telah menunjukkan aktiviti antimalaria ultrapoten ($IC_{50} = 1.5 nM$). Untuk memahami mod tindakan DHLC, profil aktiviti DHLC semasa jangkitan sel darah merah telah ditentukan berdasarkan ujian pendedahan/pembasuhan DHLC pada masa-masa tertentu. DHLC mempunyai profil aktiviti antimalaria yang berbeza (tropozoit > skizon > cincin) dengan klorokuin dan artemisinin, maka cara mod tindakan yang berbeza. DHLC juga melambatkan perkembangan parasit semasa

jangkitan sel darah merah. *P. Falciparum* yang rentang terhadap DHLC telah berjaya dihasilkan melalui pendedahan kepada DHLC secara berterusan. Penjujukan genom keseluruhan menunjukkan gen ditandakan sebagai “gen #6” merupakan satu-satunya gen yang bermutasi dalam genom strain rentang terhadap DHLC. Gen #6 mengkodkan protein transmembran yang belum diketahui. Maka, protein ini merupakan sasaran baharu untuk pembangunan agen antimalaria. Hubungan struktur-aktiviti menunjukkan bahawa pembukaan cincin tetrahydrofuran dan penyingkiran kumpulan epoksida bertanggungjawab untuk aktiviti antimalaria DHLC. Pengenalpastian DHLC boleh menyediakan agen antimalaria baharu untuk memerangi penyebaran strain rentang antimalaria yang meluas.

IDENTIFICATION OF ANTIMALARIAL COMPOUNDS AND THEIR MODE OF ACTIONS

ABSTRACT

Malaria is one of the most significant infectious diseases in the tropics, claiming around half-million lives annually, mainly due to *Plasmodium falciparum* (*P. falciparum*) infections. To date, *P. falciparum* has developed full or partial resistance towards all three classes of antimalarials, including against the artemisinin. Hence, it may jeopardize the efficacy of the current antimalarial treatment regimen, the Artemisinin Combination Therapy (ACT), in the near future. Therefore, there is an utmost need to identify a new antimalarial compound with a novel mode of action (MoA). This study mainly focused on identifying antimalarial compounds from soil microorganisms isolated from Malaysia and Japan. The crude extracts of these strains showed potent antimalarial activity in a preliminary assay against *Pf*3D7 (wild type). The crude extracts of Malaysian strains also inhibited the activity of human GSK-3 β (75 % similar to *P. Falciparum* GSK-3 (*Pf*GSK-3)). Therefore, there is a potential to identify antimalarial activity mediated by *Pf* GSK-3 inhibition, which is as a new antimalarial MoA. In addition, three new pure compounds deposited in RIKEN chemical library were also evaluated in an antimalarial reproducibility test, to select

the most potent compound(s) for MoA determination. Overall, 18 antimalarials were identified/suggested which includes (DBP) (*Pf* 3D7 IC₅₀ = 14.4 μM), nataxazole (new antimalarial agent, *Pf* 3D7 IC₅₀ = 14.7 μM) and secalonic acid F (*Pf* 3D7 IC₅₀ = 4.1 μM) (from Malaysian strain) and koranimine (IC₅₀ = ~0.01 μM) (from Japanese strain). Interestingly, *in silico* study indicates that these compounds formed hydrogen bonds with important amino acid residues on *Hs* GSK-3β (Arg87, Lys85, and Asp200, respectively) that are conserved in *Pf* GSK-3 (Arg119, Lys108, and Asp225, respectively). Hence, DBP, nataxazole, and secalonic acid F may exert antimalarial activity by inhibiting *Pf* GSK-3. Meanwhile, dihydrolucilactaene (DHLC, a new compound isolated from *Fusarium* sp. 97-94 that was deposited in RIKEN chemical library) was shown to exert an ultrapotent antimalarial activity (IC₅₀ = 1.5 nM). To understand the MoA of DHLC, its erythrocytic stage-specific activity profile was investigated based on a time-specific drug exposure/washout assay against a sorbitol-synchronized *Pf* 3D7 culture. DHLC was indicated to exert a different stage-specific profile (trophozoites > schizont > ring) than chloroquine and artemisinin, hence a different MoA. DHLC was also shown to delay parasite egression during RBC stage infection. A DHLC-resistant strain was successfully generated via continuous drug exposure. Whole-genome sequencing revealed a gene denoted “gene #6” as the only mutated gene in the genome of DHLC-resistant strain. Gene #6 was reported to encode

an unknown conserved *Plasmodium* transmembrane protein. This protein was never reported as the molecular target of any known antimalarials, hence a novel target for antimalarial drug development. Structural-activity relationship revealed that the opening of the tetrahydrofuran ring and the absence of the epoxide group in DHLC were responsible for its antimalarial activity. The identification of DHLC may provide a new drug regimen to combat the widespread of drug-resistant strains.

CHAPTER 1

INTRODUCTION

1.1 Malaria: a brief background

Malaria is a prominent mosquito-borne (*Anopheles* sp.) disease in the tropics (Lee et al., 2020; Li et al., 2020). In 2020, around 241 million malaria cases were reported in 85 malaria-endemic countries, with 627,000 deaths, a slight increase from the previous year (World Health Organization, 2021). Most deaths were recorded in Africa (96 %), especially children under five years old and pregnant women, contributed by their more compromised immunological and hormonal responses than the general adult population (Chua et al., 2021; World Health Organization, 2021).

In humans, malaria is caused by 9 *Plasmodium* parasites species belonging to apicomplexan protozoa, that require two hosts to survive, mosquito for transmission and sexual stage (in the midgut), and vertebrate (divided into liver and blood asexual stage). *Plasmodium falciparum* (*P. falciparum*) is the most prevalent and virulent species (Ansari et al., 2016) since complications of severe malaria such as cerebral malaria, anemia, acute renal failure, pulmonary edema, and bleeding are almost entirely caused by this species. These symptoms may rapidly lead to coma and death within hours or days after manifestation (World Health Organization, 2000).

Over the past decade, *P. falciparum* continues to be the most prevalent and virulent case of malaria, followed by *P. vivax* (Amambua-Ngwa et al., 2019; World Health Organization, 2021). Meanwhile, mild or uncomplicated yet persistent malaria cases are caused by *P. malariae* (Bartoloni & Zammarchi, 2012). *P. ovale curtisi* and *P. ovale wallikeri* (closely related but distinct malaria parasite species) received the least attention as it is considered uncommon and only causes mild infection. Although *P. ovale* infection can be easily treated with chloroquine, it can evolve into a more severe or fatal strain (Mueller et al., 2007; Lau et al., 2013). In recent years, *P. knowlesi* (a zoonotic *Plasmodium*) has been the prominent cause of malaria in Southeast Asia (SEA), especially in the east of Malaysia (Zaw & Lin, 2019; Cooper et al., 2020). Moreover, possible infection from the other zoonotic *Plasmodium* species (*P. inui*, *P. cynomolgi* and *P. coatneyi*) has been reported in Malaysia (Yap et al., 2021).

1.2 Problem statement

1.2.1 Drug resistant development

SEA continues to be the hotspot for the emergence of strains resistant against frontline antimalarial starting with CQ (1957) and sulphadoxine-pyrimethamine resistance strains (in the 1960s) (Trape, 2001; Roper et al., 2004; Singh & Sharma, 2016; Bushman et al., 2018). The resistance emergence is mainly driven by poor quality antimalarials widely used in SEA (Dondorp et al., 2004; Nayyar et al., 2012).

More than 40 % of antimalarials sold in SEA are either did not contain any active ingredients or contained <10 % of the active compounds (Dondorp et al., 2004). The subtherapeutic dosage increases the risk of resistance emergence (prolonged drug exposure), which eventually favors the selection/spreading of the resistance strains (Newton et al., 2006).

As a consequence, the ART-resistant strains have emerged in SEA since 2009 and recently in Africa (2019) (may also be due high use of counterfeit drugs) (Nayyar et al., 2012; Boddey, 2017; Tahghighi et al., 2020; Balikagala et al., 2021). Its emergence in Africa will likely cause a malaria outbreak if proactive actions to curb the spreading are not taken since ART is the final effective frontline antimalarial drug (Ouji et al., 2018; World Health Organization, 2021).

1.2.2 Low antimalarial drug diversity

Although natural and synthetic antimalarials were introduced in the late 1800 and 1940s, only a small number of compounds reached the clinical stage (Grimberg & Mehlotra, 2011). Moreover, these compounds belong to only three broad classes; aryl amino alcohol compounds, antifolate compounds (Luzzatto, 2010), and ART compounds (White, 2008; Patrick, 2020). Since *P. falciparum* has developed resistance phenotypes against all classes of antimalarials, new drug classes that exert

a different mode of action (MoA) than the existing drug regimen need to be explored for effective treatment (Flannery et al., 2013; Burrows et al., 2017).

1.2.3 Antimalarials with unknown MoA

Determining the exact target of a drug is valuable knowledge as it can prevent late-stage failures that increase the chances of drug approval. In general, information on the actual target leads to better dosing, monitoring potential side effects of a drug, and stratifying better clinical trials on suitable patients. Hence, many promising drugs failed at an early stage trial due to cytotoxic activity, considering a wide array of cell signaling processes, enzymes, and isoforms functioning in the human system, (Medina-Franco et al., 2013; Peters, 2013).

Similarly, most frontline antimalarials were developed without knowing their target since antimalarial therapeutic potency was primarily identified via cell-based assay (Fidock et al., 2004; Schlitzer & Ortmann, 2010). As a result, it is difficult to establish hit optimization due to pharmacokinetics or toxicological issues (Hallyburton et al., 2017). For example, primaquine is the only clinically approved antimalarial that can eliminate hypnozoite to date. However, since primaquine's target is unknown, further studies have been limited only to related analogs such as tafenoquine (Vale et al., 2009). Therefore, a drug with a known MoA is preferable for the next generation of antimalarials.

1.3 Strategies to solve malaria-associated problems

1.3.1 Drug discovery from nature

Natural products are genetically encoded in the genome of their producer, resulting from the evolution via natural selection. The products are usually beneficial to the producer as they are produced to engage with their respective biological targets. Hence, natural products are naturally equipped with chemical features required for biological activity, such as higher counts of chiral centers, sp³-hybridized carbon and oxygen content, low nitrogen and aromatic rings, and larger macrocyclic aliphatic rings. These features create complex 3-D structures and are stereochemically superior to synthetic compounds to effectively interact with biological components (Rodrigues et al., 2016).

Plant natural products are a rich source of prolific antimalarial compounds with unique structures. The first antimalarial was quinine, isolated from cinchona bark (*Cinchona cordifolia*) in 1820 and fully synthesized in 1854. Quinine remained in the frontline regimen until replaced by CQ in the 1940s. A few decades later, ART was identified from sweet wormwood (*Artemisia annua*) as another plant-based antimalarial. ART bears a sesquiterpene lactone with an endoperoxide group, a unique natural product structure that is responsible for ART antimalarial activity (Dagen, 2020). Although numerous experimental antimalarials were continuously reported

from plants such as 3,4,5-tri-*O*-caffeoylquinic acid (Nugraha et al., 2022) (*Pluchea indica*) and 8 β ,13 β -kaur-15-en-17-ol (*Podocarpus polystachyus*) (Amir Rawa et al., 2022), in recent years, no plant-based antimalarials even reached preclinical tests (Saha et al., 2022).

One of the significant problems with plant natural products is the low production of active compounds (including artemisinin) since external factors such as sampling location and environmental factors may influence the recovery rate of the natural products. Although synthesis of the active compound could solve the problem, unfortunately, not every compound can be produced via total synthesis (Katiyar et al., 2012). To overcome this problem, larger quantities of samples are needed to acquire enough pure compounds, which will increase the production cost (Habibi et al., 2019). Often, this problem cause plant-based antimalarials to be economically impractical for development and commercialization. It will also provide a market for counterfeit drugs, especially in less-developed regions (Karunamoorthi, 2014).

Since the discovery of microorganisms as a prolific source of active compounds in the 1920s, microorganism-derived compounds have been used extensively in biopharmaceutical sectors, scientific research, food industry, and agriculture (Sanchez-Garcia et al., 2016; Pham et al., 2019). The ability to culture them under controlled parameters or to be engineered to activate silent genes in the

laboratory gives microorganisms an edge over plants for the mass production of new active compounds (Song et al., 2015; Pérez-Moreno et al., 2016; Matsumura et al., 2018; Wright, 2019). Therefore, microbial natural products are an excellent source to search for new antimalarials.

1.3.2 Targeting host enzymes

Antimalarials targeting host enzymes are an attractive therapeutic strategy to prevent resistant development. It is because, unlike viruses, parasites cannot mutate enzymes encoded in the host genome since no genome integration occurs between *Plasmodium* and humans during their life cycle (Fidock et al., 2004; Kesely et al., 2016). For instance, Band 3 (AE1, SLC4A1, anion transporter) and ankyrin are predominant erythrocyte membranes. It maintains red blood cell (RBC) integrity via connecting the cell membrane to its cytoskeleton (Anong et al., 2009; van den Akker et al., 2010).

Tyrosine phosphorylation of band 3 causes detachment of ankyrin, destabilizing the RBC membrane and leading to hemolysis (Ferru et al., 2011; Pantaleo et al., 2011). Interestingly, *P. falciparum* infection stimulates a significant increase in band 3 tyrosine phosphorylation despite the absence of tyrosine kinase in *P. falciparum* kinome (Pantaleo et al., 2010). It indicates that *P. falciparum* utilizes host

tyrosine kinase (activating) to facilitate its egression from ring to trophozoites and schizont. The weakened cell membrane finally ruptured towards the end, releasing merozoites and infecting new RBC (Kesely et al., 2016).

Through drug repurposing (a process of finding new medical uses for existing drugs/compounds), imatinib (Food and Drug Administration (FDA)-approved tyrosine kinase inhibitor to treat cancer) was identified as a potent antimalarial that reached phase II in a clinical trial. Imatinib inhibits erythrocyte tyrosine kinase activity that causes parasite entrapment and termination (Talevi & Bellera, 2020; Chien et al., 2021). Hence, targeting host enzymes paired with drug repurposing is a powerful approach moving forward in antimalarial development. It offers a lower failure rate as the repurposed drug has already been tested for human safety (Pushpakom et al., 2019).

1.3.3 Targeting essential cell components for *Plasmodium* survival

A recent PiggyBac mutagenesis analysis uncovers numerous cell components that can be targeted to develop antimalarial agents against *P. falciparum*. The AT-richness of the *P. falciparum* genome was exploited to generate over 35,000 *P. falciparum* mutants. These mutagenesis lead to the identification of essential genes (non-mutable genes). Eventually, almost 3,500 essential genes were identified for *P.*

falciparum *in vitro* asexual blood-stage growth (Zhang et al., 2018). Hence, numerous unexplored malarial parasite cell components can be targeted for drug development.

1.4 The rationale of the study

In this study, antimalarial compounds from microbial sources were explored, and the MoA of the most potent compound(s) was determined as an effort to identify new malaria treatment that may curb the spreading of drug-resistant *P. falciparum*. It may prevent major malaria breakout and enrich our knowledge of the parasite's biology (Weiwer et al., 2010; World Health Organization, 2021).

1.4.1 Soil actinomycetes, an inexhaustible source for bioactive compounds

As of 2020, around 75,000 bioactive compounds originated from natural resources were identified, by which microorganisms (actinobacteria/actinomycetes, fungi, and eubacteria) are the major contributor with 34,000 (46 %) of bioactive compounds, followed by plants (higher and lower plants) (31,000), marine invertebrates (10,000) and terrestrial animals (1,000). Soil actinomycetes are known as an inexhaustible source of bioactive compounds. Out of ~2000 genera, only *Streptomyces* is well studied (easy to be cultured in the laboratory) for drug discovery as 60 % of bioactive compounds from actinobacteria were identified from this genus

alone. Hence, more bioactive compounds are to be discovered from the underexplored genus or the “rare actinomycetes” (Ding et al., 2019).

Soil microorganisms, significantly contribute to natural drugs due to their high therapeutic index and significant pharmacological activities (Adegboye & Babalola, 2013). In addition, compounds from soil microorganisms are an excellent natural product source of antimalarial agents due to; 1) their sizeable structural diversity, and 2) they are still not widely explored for the discovery of antimalarial drugs (Pérez-Moreno et al., 2016). The type of forests was suggested to determine soil actinomycetes distribution and the variety of secondary metabolites produced since their growth are influenced by organic materials mainly from plants (Hackl et al., 2005; Ghorbani-Nasrabadi et al., 2013; Tripathi et al., 2016; Law et al., 2019; Mahmud et al., 2022).

Tropical forests are regarded as the best sampling location for drug discovery, hence known as the “world’s largest pharmacy” (Guariguata et al., 1998; Temu, 2015). As part of Borneo Island, Sabah is one of the twelve mega biodiversity hotspots globally. More than ten forest types can be found in Sabah, which covers approximately 60 % of its landmass (Kulip et al., 2010; Payne, 2011; Yen et al., 2021). In general, 15,000 plant species were recorded in Borneo, of which 34 % are endemic species (WWF, 2022). Hence, the existence of diverse species of flora and fauna in

Sabah, Malaysia, may lead to the isolation of novel strains and bioactive compounds resulting from soil actinomycetes-plant interaction.

In a previous study, more than 1000 culturable actinomycetes strains were isolated from different forest types of Sabah. Some of these strains showed potent activities against human glycogen synthase kinase-3 (*Hs* GSK-3 β) and malaria parasite, *P. falciparum* 3D7 strain (*Pf* 3D7, wild type (WT)) (Mahmud et al., 2022). The most potent strains were selected to identify active compounds in this study. To further diversify the tested scaffolds, microbial strains isolated from Japanese soils and synthesized compounds deposited at the Chemical Biology Research Group (CBRG) at Rikagaku Kenkyusho (RIKEN) microbial and chemical libraries were evaluated for their antimalarial activities. In addition, a series of new lucilactaene derivatives, a biosynthesis product of *Fusarium* sp. 97-94, was also tested for their activity against *Pf* 3D7. Lucilactaene is an interesting antimalarial drug lead that was previously reported with potent antimalarial activity (Kato et al., 2020).

1.4.2 *Hs* GSK-3 β inhibitor may lead to identifying new antimalarial compounds, a target-based approach.

Previously, a yeast-based assay system utilizing a mutant yeast strain expressing *Hs* GSK-3 β was applied to screen for *Hs* GSK-3 β inhibitors from soil microorganisms and plant extracts of Sabah (Cheenpracha et al., 2009; Ho et al., 2009).

It was shown that most of the active extracts also exert potent antimalarial activity with no cytotoxic effect against Chang's liver cells. Notably, these samples also were indicated to inhibit host GSK-3 activity of *P. berghei* infected mice in the liver (Dahari et al., 2016). Hence, dual inhibition of host and parasite GSK-3 is an exciting approach in malaria treatment.

Based on these premises, the potential of using mutant yeast expressing *Hs* GSK-3 β as a preliminary assay to narrow down the sample for the antimalarial activity was further evaluated. The crude extracts that showed potent inhibitory activity against *Hs* GSK-3 β and *Pf* 3D7 were subsequently fractionated to identify the active compounds.

1.4.3 Spontaneous drug resistance development, an effective strategy to identify the antimalarial molecular target

The development of drug resistance ability in *Plasmodium* has been described as unique compared with other infectious diseases. They can induce exact resistance in the cellular target of the antimalarial drugs instead of random mutations (Goldberg et al., 2012). Although the precise mechanisms are still not clearly defined, resistance in *Plasmodium* has a genetic basis (Sibley, 2015). Hence, the molecular target of antimalarials can be identified via generating drug-resistance parasites in the laboratory, then comparing the genomes of the resistant clones to the WT (Meister et al., 2011). This method has led to the identification of numerous novel targets,

including *Pf*ATP4 and *Pf*CARL (Crowther et al., 2011). In this study, the spontaneous mutation approach was applied via continuous drug exposure; a) to identify the MoA/molecular target of compounds identified/deposited in RIKEN and b) to confirm if active compounds identified from the target-based approach can be confirmed via the generation of mutant *Pf*GSK-3.

1.5 Research objectives

1.5.1 General objective

The study aimed to assess antimalarial potential of soil microorganisms and to explore new chemical scaffolds, possibly with a different mode of action than the current antimalarial frontline.

1.5.2 Specific objectives

- i) To evaluate the antimalarial activity of crude extracts previously identified as *Hs* GSK-3 β inhibitors via *in vivo* yeast-based assay from Malaysian soil microorganisms.
- ii) To identify antimalarial compounds produced by Malaysian and Japanese soil microorganisms.
- iii) To determine the antimalarial MoA of the most potent antimalarial compounds in this study.
- iv) To predict the importance of the antimalarial molecular target of the most potent antimalarial compound in this study via stage-specific activity evaluation.
- v) To establish the structure-activity relationship of the most potent antimalarials identified in this study.

CHAPTER 2

LITERATURE REVIEW

2.1 Brief historical data on malaria

Malaria is an ancient infectious disease that remains endemic in the tropics until today. The term “malaria” was derived from medieval Italian words “mal (bad)” and “aria (air)” due to the connection of this disease with the swamp area in Italy. However, the origin of this disease can be traced back to Egyptian papyrus (3,500 BC), The Chinese Canon of Medicine, *Nei Ching* (3,000 BC), ancient Indian sculptures (1,000 BC), and Cuneiform tablet in Mesopotamia (500 BC), all describing fever associated with rigors and enlarged spleen, certainly attributed to malaria (Bruce-Chwatt, 1988). Meanwhile, malaria spread into Europe, Scandinavia, and Britain during the Neolithic Period (~4,000 BC) via the Nile Valley (Carter & Mendis, 2002; Suh et al., 2004; White, et al., 2014; Piperaki & Daikos, 2016; Dagen, 2020).

A more detailed description of malaria was recorded by Celsus in 1 AD (a Roman writer), who described three types of malaria fever in *De Medicina* as quartan, tertian, and lethal semitertian fevers. These malarial fevers are now known to be inflicted by *P. malariae*, *P. vivax*, and *P. falciparum*, respectively (Cox, 2002). However, the *Plasmodium* parasites were not identified until almost 2,000 years later. Giovanni Lancisi was one of the first to suggest the relation between swamp areas and

mosquitoes with malaria in 1716 (Italy) as the draining of the swamp area reduced malaria cases and suggested that mosquitoes spread the disease. Lancisi also performed a postmortem study on the body of a periodic fever victim and identified a dark-colored pigmentation in the tissue (Klaassen et al., 2011). In 1847 Rudolph Virchow (Germany) confirmed that the colored pigmentation observed by Lancisi in 1716 came from the blood (Brabin, 2021).

Almost 30 years later, the causative candidates of malaria were finally proposed. First, in 1878, Corrado Tommasi-Crudell and Theodor Klebs proposed a bacterium (named *Bacillus malariae* (*B. malariae*)) isolated from Pontine Marshes, a former marshland in Italy, as responsible for malaria. This assumption was based on symptoms such as fever and spleen enlargement observed in *B. malariae*-injected rabbits (Haas, 1999). At about the same time, Charles Laveran, a French military doctor, performed a postmortem of patients who succumbed to malaria in Algeria. At first, Laveran observed pigmentation in organs and tissues as previously reported by Lancisi but failed to determine the cause. He then examined wet blood film (without staining) of leukocytes and erythrocytes and observed pigmented cells. Upon further inspection, he also discovered spherical and crescent-shaped (now known as the *Plasmodium* gametocytes) bodies containing pigment in those cells (Tan & Ahana, 2009; Dagen, 2020).

In 1880, Laveran observed pigmented spherical bodies with flagella-like structures in the blood of malaria patients that were motile and capable of infecting new RBC. He also found that the crescents can be removed when treated with quinine (the first antimalarial compound purified from the bark *Cinchona cordifolia* in 1820). Based on his study, two monumental findings were obtained: 1) Laveran reported parasite (initially named *Oscillaria malariae* (*O. malariae*)) as the causative agent of malaria, a remarkable finding on its own as it was the first protozoan parasite ever identified in humans, and 2) he proposed possible egression of the parasite in blood and its pathological implication. First, a clear spot was observed in RBC upon infection. Then, the spot grows and acquires the pigment until the erythrocyte ruptures, which causes fever in malaria patients (Cook, 2007; Dagen, 2020).

Laveran's finding was met with many oppositions, including from distinguished scientists such as Louis Pasteur and Robert Koch, because the "parasite" observed by Laveran was possibly the breakdown product of RBC. Hence, the idea of *B. malariae* as a malarial causative remained accepted until 1884. However, in the same year, Pasteur was finally convinced and supported Laveran's proposal once he directly observed the motile and flagellated spheres under the microscope (Brey, 1999). In 1884, Ettore Marchiafava and Angelo Celli identified a distinct structure to the one observed by Laveran, characterized as an active "amoeboid ring" (now known as the

ring stage). They thought it was an entirely different microorganism and was named *Plasmodium*, which eventually overrides *O. malariae* (Garnham, 1988; Dagen, 2020).

In 1885, Camillo Golgi identified two distinct species of parasite protozoa; *P. malariae* (responsible for quartan fever) and *P. vivax* (that cause tertian fever) (Tognotti, 2007). In 1890, Marchiafava and Golgi made another breakthrough discovery as they identified *P. falciparum*, which also causes tertian fever but is more fatal than *P. vivax*. Hence, *P. falciparum* is accounted as the cause of malignant tertian fever, while *P. vivax* causes benign tertian fever (Capanna, 2006). In 1894, Laveran (now associated with Pasteur Institute) stated that he had failed to find malaria parasites in the water, air, or even soil. Hence, he believed that *Plasmodium* might exist in another host outside humans. Laveran suggested the mosquito as another *Plasmodium* host, based on Patrick Manson's finding in 1877 that the mosquito spread filarial worms, acting as its vector (Dagen, 2020).

Findings made circa 1900 have an unprecedented impact on malaria study during the postmodern era that further enriched scientific understanding of *Plasmodium* infection treatment, vector control, and biology (Cox, 2010). In 1934, IG Farbenindustrie developed a series of antimalarial based on the structure of quinine, including CQ (4-aminoquinolines), a frontline antimalarial drug in the 1950s before the emergence of the CQ-resistance strain. Meanwhile, the life cycle of the

Plasmodium parasite was finally understood in the early 1980s (Krotoski et al., 1982; Josling & Llinás, 2015), which led to a new drug regimen by pairing drugs targeting different *Plasmodium* life stages and MoA (Nosten & White, 2007).

2.2 *Plasmodium* and its life cycle

In general, *Plasmodium* parasites require two hosts to complete their life cycle. The first host is *Anopheles* sp. mosquito, vital for *Plasmodium* sexual diploid cycle (in the midgut) and acts as their transmission vector (haploid sporozoites in salivary glands) to infect their second host (vertebrates such as mammals, reptiles, or birds), for the haploid asexual cycle (Henriquez, 2020). Almost 40 *Anopheles* sp. mosquitoes are known to transmit *Plasmodium* parasites to humans (Nicoletti, 2020). *Anopheles gambiae* was identified as the most efficient vector responsible for spreading *P. falciparum* (Koella et al., 1998).

In humans, *Plasmodium* asexual life cycle is divided into exoerythrocytic (in the liver) (Vaughan & Kappe, 2017) and intraerythrocytic (in the RBC) (Wallqvist et al., 2016) stages. Saliva injected by an infected mosquito will transfer sporozoites into the bloodstream and enter liver cells. The entry of sporozoites into the hepatocytes is highly precise due to the circumsporozoite protein that bears a ligand that only binds specifically to the liver basolateral domain (hepatocyte cell membrane). The entry of sporozoites will initiate the asexual reproduction, known as the pre-erythrocytic cycle

(PE) or primary exoerythrocytic schizogony (EE) stage. Sporozoites then metamorphose into trophozoites and transform into schizont and merozoites through schizogony (Ménard et al., 2008; Duffy et al., 2012; Teixeira et al., 2021).

The erythrocytic cycle starts once merozoites leave the liver cell to penetrate RBC. During the invasion, the merozoites initiate invagination of the RBC membrane to form a membrane sack known as parasitophorous vacuole (PV) (Koch & Baum, 2016). Although the function of PV is not fully understood, it is known to act as an intraerythrocytic shelter necessary for nutrient acquisition (Bullen et al., 2012), facilitate the export of virulence factors (Pellé et al., 2015) and subcompartmentalization (Adisa et al., 2003; Matz et al., 2020).

Within this capsule, the merozoites transform into trophozoites (early trophozoites or ring-stage and late trophozoites). Next, the late trophozoites developed into blood-stage schizont. They were released from ruptured RBC together with metabolic waste and residual bodies to stimulate the release of macrophages and cytokines responsible for synchronous fever, a common malaria pathology. After an indeterminate number of asexual cycles, some of the merozoites will enter erythrocytes and become macro- and microgamonts to be ingested by the mosquito for sexual reproduction, and the cycle is repeated (Henriquez, 2020) (Figure 2.1).

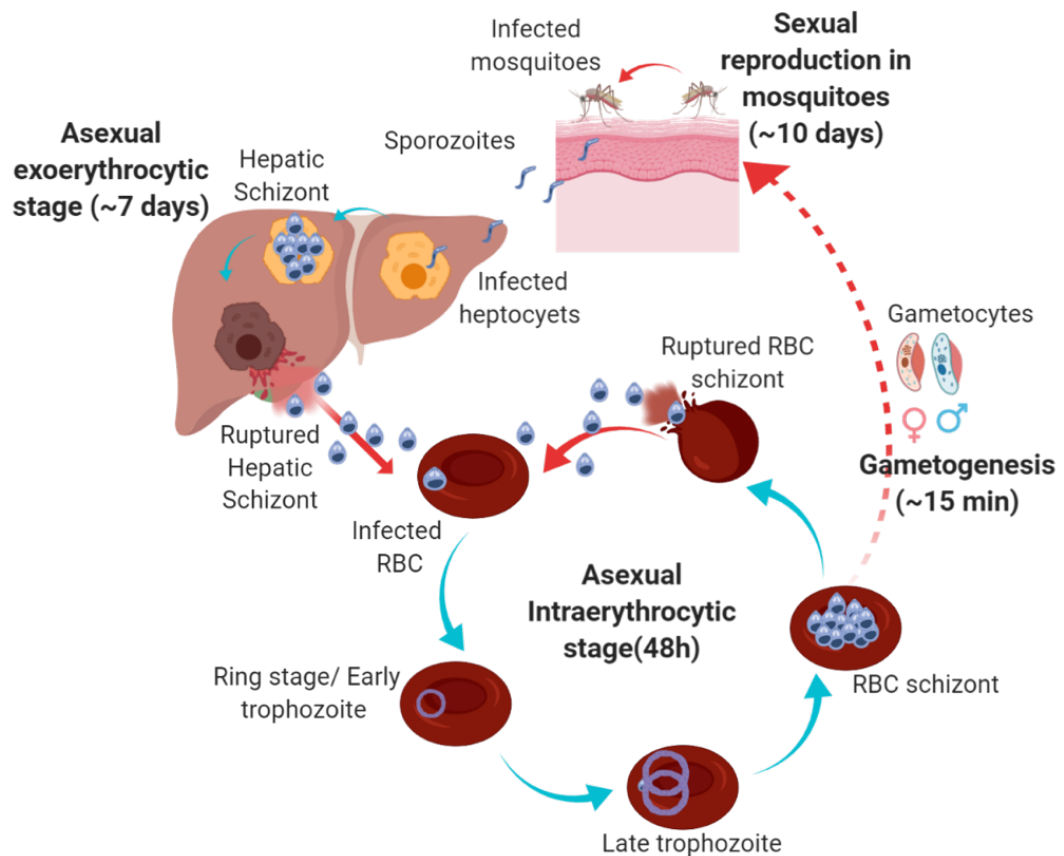


Figure 2.1 The life cycle of *P. falciparum* (Matthews et al., 2018).
Created with BioRender.com

2.3 Druggable stage of *Plasmodium* life cycle

Based on the *Plasmodium* life cycle, different life stages can be targeted to develop antimalarial drugs, such as targeting asexual and sexual stages (Wadi et al., 2019), hypnozoites (dormant schizont stage)/liver stage (Derbyshire et al., 2011), and transmission-blocking (Birkholtz et al., 2022). However, most of the antimalarial act during *Plasmodium*'s RBC life cycle since the screening requires the least labor and specialized material. Besides, an extensive compound library can be tested simultaneously. Hence, the RBC stage will continue to be the main target in drug development. (Gamo et al., 2010; Meister et al., 2011; Baragaña et al., 2015; Vos et

al., 2015; Swann et al., 2016). Antimalarial agents known to inhibit *Plasmodium* at the RBC stage are CQ, amodiaquine, quinine, sulfadoxine-pyrimethamine, ART and its derivatives, and lumefantrine (Zarchin et al., 1986; Loria et al., 1999; Joof et al., 2021; Famin & Ginsburg, 2002; Krishna et al., 2004).

CQ and ART are the most effective antimalarial compounds identified so far. Both compounds exert a unique MoA and can target a broad range of essential biochemical functions in *Plasmodium*. CQ is a weak diprotic base found in three forms in cells (un-protonated, mono-protonated, and di-protonated). The un-protonated form of CQ is a membrane-permeable form that can diffuse into the infected erythrocyte and digestive vacuole (DV) (lysosomal isolated acidic compartment formed by *P. falciparum* in erythrocytes) (Slater et al., 1991; Ehlgen et al., 2012).

In RBC, *Plasmodium* continues to multiply by ingesting the host cell cytosol into peptides and heme. Heme is a toxic material to *Plasmodium* and must be converted into an inert and harmless crystalline polymer hemozoin (malaria pigmentation) and deposited in the DV (Slater et al., 1991; Ehlgen et al., 2012). Once inside the DV un-protonated CQ become protonated (not permeable) and trapped in the DV (Homewood et al., 1972; Yayon et al., 1984). Protonated CQ binds with haematin (oxidized heme), preventing its further conversion into hemozoin crystal which eventually damages the *Plasmodium* membrane (Sugioka et al., 1987; Bray et al., 1998; Pagola et al., 2000).

Meanwhile, ART is a highly effective antimalarial agent as it affects *Plasmodium* at all stages of growth and acts on multiple targets (Ismail et al., 2016). In the infected RBC, ART become activated from the bond cleavage of its endoperoxide bridge by Fe²⁺-heme (originated from hemoglobin degradation by *Plasmodium*). In this form, ART is lethal to the parasite due to biomolecules alkylation (heme, protein, and lipids) that cause oxidative stress and cellular damage (Tilley et al., 2016). It now becomes clear that the activity of ART is directly proportional to the amount of Fe²⁺-heme. It makes ART unique compared with most antimalarial as it also can kill *Plasmodium* at the early ring stage (hemoglobin degradation begins with several hours of RBC invasion) (Portugaliza et al., 2020).

ART antimalarial activity is at its peak during trophozoites as hemoglobin catabolism at the highest rate (Klonis et al., 2013; Xie et al., 2016). It can also reduce 10,000-fold *Plasmodium* every 48-72 hours, providing rapid clearance but having a short half-life (thus requiring the second drug for complete *Plasmodium* elimination). Moreover, ART has a consistent antimalarial activity that is reproducible, wide therapeutic index, and low toxic effect on human cells (Dondorp et al., 2009; Maude et al., 2010; White et al., 2014).

2.4 Malaria: an ongoing battle

Despite numerous efforts to eradicate the *Plasmodium* parasite, malaria remains one of the most widely spread and fatal diseases today. More than 200 million new clinical cases with half a million death have been reported annually over the past two decades (Cibulskis et al., 2016; World Health Organization, 2021). Overall, malaria cases were reported to be increasing in 2020 (World Health Organization, 2021). Modeling analysis suggested that the increase was contributed by COVID-19. The pandemic indirectly disrupts malaria treatment and prevention worldwide (Weiss et al., 2021). In addition, a more worrying development was reported in certain regions, such as Laos, by which malaria cases have been steadily increasing since 2012, possibly linked to the emergence of drug resistance malaria (Imwong et al., 2015).

Moreover, only three broad classes of chemicals were identified as the antimalarial agent in clinical use. They are arylamino alcohol compounds, antifolate compounds, and ART compounds. The MoA exerted by these drugs can be divided into three mechanisms which are tissue schizonticides (primaquine), blood schizonticides (CQ, ART, quinine), and sporonticides (proguanil, pyrimethamine) (Cui et al., 2015).